Blueprints for inorganic materials with natural form: inorganic liquid crystals and a language of inorganic shape †

Neil Coombs, Deepa Khushalani, Scott Oliver, Geoffrey A. Ozin,* Guo Cheng Shen, Igor Sokolov and Hong Yang

Materials Chemistry Research Group, Lash Miller Chemistry Department, University of Toronto, 80 St. George St., Toronto, Ontario, Canada M5S 3H6

The form problem in biomineralization and biomimetic inorganic materials chemistry is morphogenesis, the origin and control of shape. In this article, an overview of an inorganic liquid crystal based paradigm for constructing inorganic shape is provided. The synthesis of mesoporous silica and mesolamellar aluminophosphate morphologies with 'natural' form is presented. Macroscale shapes and patterns of these materials result from the polymerization, curvature and growth of a silicate liquid crystal mesophase or a phosphate liquid crystal microemulsion. Recent novel examples, such as, micelle templated oriented mesoporous silica films, self-assembled monolayer patterned mesoporous silica, vesicle templated macroporous silica and mesoporous silica molded polymer mesofibres that exploit this paradigm of synthesizing shape are also presented. The time is right to explore morphogenesis in order to provide advanced materials where control of structure over all length scales determines properties and function.

Morphogenesis is concerned with the origin and control of shape in biomineralization and biomimetic inorganic materials chemistry. Biomineralization centers around the idea that organics control the nucleation, growth and form of inorganics, and it is this process that creates hierarchical composite structures with unusual chemical and physical properties where form determines function.[1] Likewise, biomimetic inorganic materials chemistry aims to exploit the principles of biomineralization to synthesize novel inorganic materials where morphology guides applications.[2]

Nature is frugal in her choice of inorganic materials, generally restricting herself to calcium phosphate, carbonate and oxalate, silica and iron oxides.[3] However, the mineralized designs and diversity of naturally occurring forms have rarely been equaled in synthesis until recently.[4–6] The chemical bonding of biominerals is not unusual and varies from amorphous covalent networks found in silica objects to multi-crystalline ionic calcium-based shapes. These structures are used in, for example, protection and support, as sensors and for regulation of inorganic nutrients.[7] In molecular terms, it is easy to comprehend the early stages of self-organization, molecular recognition, nucleation and vectorial growth that usually precede the morphogenesis of biomineral form. It is not obvious however, how complex shapes emerge and how, in turn, they can be copied synthetically.

Biological materials display hierarchical organization of structure. At each level of this hierarchy, distinctive building rules are apparent. Some of these levels do not demand periodicity in the definition of ideal crystals and their description requires a break from standard crystallography.[8] The traits of biological minerals are manifested by an astonishing array of curved shapes, surface patterns and hierarchical order. These are not the characteristics of conventional crystals with their limited range of polyhedral habits and similar rules of construction from atoms to bulk.[9] A shift from the theory of exact equivalence and long-range order in the perfect crystal, to quasi-equivalence and short-range order in biological 'crystals' is necessary. To expand, the symmetry elements of the 230 space groups determine the number of ways that identical atoms can be arranged in an infinite array. Here, the underlying space pattern of the primitive unit cell dictates the shape of a crystal.[9] To deal with systems whose shape does not conform to this stereotype, it is necessary to abandon the idea that the environment of every lattice site has to be identical for order to emerge, and to consider ways of introducing curvature into morphology.[8,10,11]

The self-organization properties and mineralization chemistry of inorganic liquid crystals appear to be the key to understanding morphogenesis of inorganic shape. The inspiration for this idea stemmed from the discovery in 1992 by Kresge *et al.*[12] of silicate liquid crystal mesophases (MCM41S), analogous to the well known organic lyotropic versions. This subsequently led to the synthesis of mineralized (*i.e.*, fossilized) replicas of aluminophosphate and silica liquid crystal phases.[13,14] These materials exhibited extraordinary morphologies with 'natural' form. The inorganic region of these shaped materials was amorphous yet it managed to partition space into periodic mesoscale patterns of pores, channels and lamellae. Since this work, there has been a flurry of interest in morphosynthesis[5,15–25] and a new and exciting field of inorganic materials chemistry appears to be emerging.

In this article, we describe the mineralization of silicate and phosphate liquid crystals to create morphologies with 'natural' form. By 'natural' form, we loosely imply the visual perception of spatial images of a class of objects which share particular features that are typically associated with biological shapes. The rudiments of a nucleation and growth model that explains morphogenesis of shape in these inorganic liquid crystal systems will be presented. The potential of developing the science of synthetic morphology for advanced materials technologies is illustrated by recent work involving macro- and meso-scale designs. Experimental details of this research are to be found in the cited references.

Aluminophosphate Morphologies

The initial idea that intricate inorganic shapes could be synthesized originated with surfactant-templated aluminophosphate materials.[13a] The synthesis comprised of alumina, phosphoric acid and decylamine in a tetraethylene glycol [$O(CH_2CH_2OCH_2CH_2OH)_2$, TEG]–water co-solvent system.

---

† Based on the presentation given at Dalton Discussion No. 2, 2nd–5th September 1997, University of East Anglia, UK.
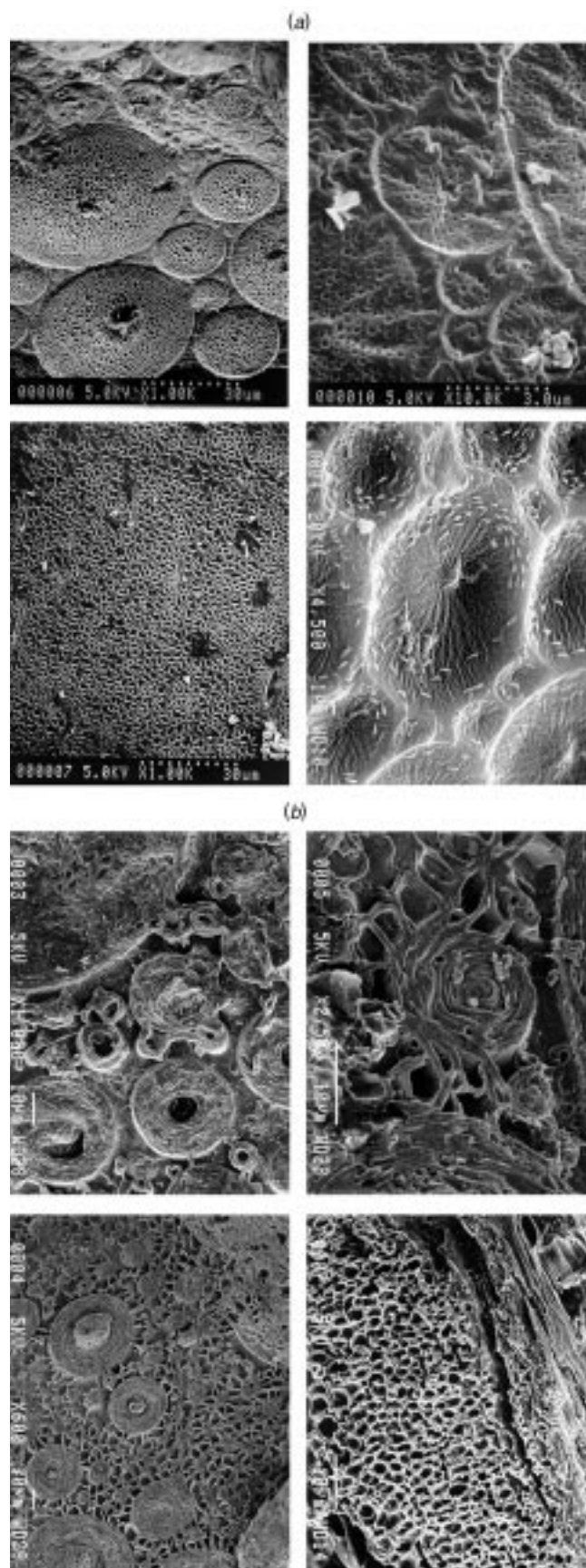
Fig. 1 Scanning electron microscopy images of representative mesolamellar aluminophosphate synthetic morphologies (a) synthesized with TEG, H_2O, H_3PO_4, decylamine and (b) synthesized with TEG, paraffin oil C_8–C_{22} alkane, H_2O, H_3PO_4, decylamine

Millimeter sized inorganic spheroids and hollow shells bearing micron dimension surface patterns (e.g. pores, bowls, star dodecahedra) were observed through scanning electron micro-

Fig. 2 Transmission electron microscopy image showing the mesolamellar structure of the aluminophosphate morphologies (scale bar: 30 nm)

scopy (SEM). The resemblance of the morphologies to radiolaria and diatom microskeletons was impressive, Fig. 1(a). Powder X-ray diffraction (PXRD) and transmission electron microscopy (TEM) images of sectioned samples established aluminophosphate layers separated by decylammonium lamellae with a d_{001}-spacing of ca. 30 Å, Fig. 2. Elemental analysis and thermogravimetric analysis (TGA) defined an Al:P ratio of about 1:2 and an organic and water content of about 45 and 5 wt. %, respectively. The lamellar structure displayed mesoscale but lacked microscale order.

Two key aspects of the synthesis of these morphologies were noted. One was the templating behavior of a decylammonium dihydrogenphosphate (DDP) liquid crystal phase. A single-crystal X-ray diffraction (SCXRD) structure of DDP,[13a,b] recrystallized from water, revealed a network of interdigitated decylammonium cations arranged orthogonally and intricately hydrogen-bonded to a layer of dihydrogenphosphate counter anions, Fig. 3. The second was the behavior of the solvent. Tetraethylene glycol served a multifunctional role: as a co-solvent with water, a polydentate ligand for Al[III], and a co-surfactant for inducing bilayer curvature.[13,16,17,19,26]

It was established from variable-temperature PXRD and differential scanning calorimetry (DSC) that DDP and DDP–TEG displayed smectic liquid crystal properties at the reaction temperatures required to template the aluminophosphate morphologies.[13c] Subsequently, variant mixtures of the individual components of the TEG–water–phosphoric acid–decylamine synthesis system were investigated using a variable-temperature attachment of a polarizing optical microscope (POM).[13c] This provided direct in situ images of the species responsible for the growth of the surface patterned morphologies. In essence, close-packed micron scale cellular-shaped objects displaying smectic liquid crystal behavior and characteristic optical birefringence textures spontaneously appeared from an initially homogeneous solution under the conditions that yielded the aluminophosphate morphologies.
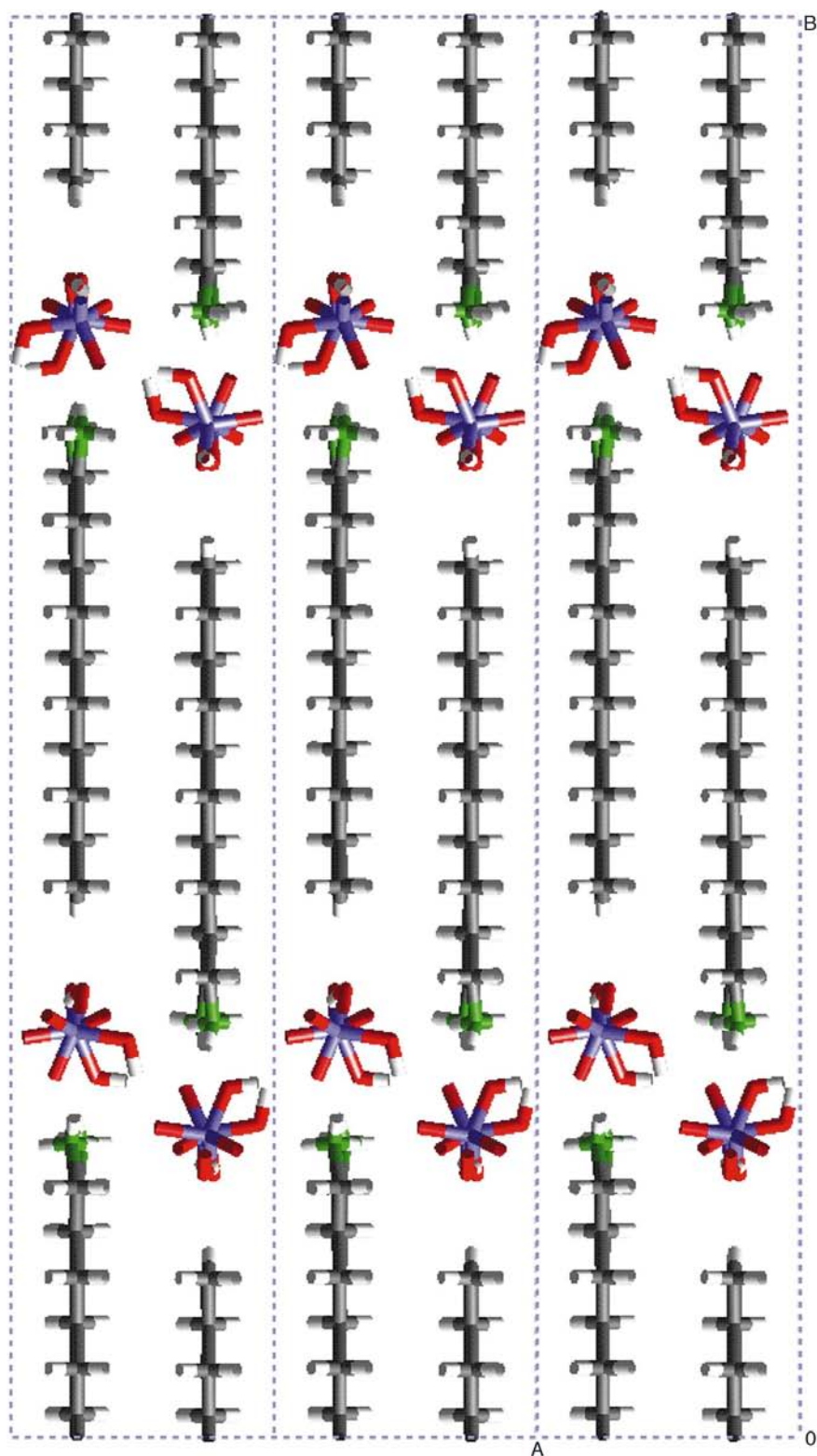
Fig. 3 Single-crystal X-ray diffraction structure of the lamellar decylammonium dihydrogenphosphate template. The dihydrogenphosphate anions form hydrogen-bonded layers sandwiched between interdigitated bilayers of the decylammonium cations

It is inferred that these objects are phase separated water–DDP–TEG and/or air–DDP–TEG smectic liquid crystal microemulsions, Fig. 7. These foam-like structures behave as the precursors most likely responsible for the formation of solid and hollow multilayer aluminophosphate spheroidal shapes.[26] It is known that alumina reacts with glycols to form aluminoglycolate anions.[27] Therefore, the aluminium precursor in the system is most probably a glycol soluble Al^{III}–glycolate complex. This species diffuses from the glycol regions to the DDP liquid crystal interface, where it reacts with the dihydrogenphosphate counter anions to form the lamellar alumino-

phosphate. Since condensation-polymerization of protonated phosphate and hydroxy aluminium species, that is, $\equiv POH + \equiv AlOH \longrightarrow \equiv P-O-Al\equiv + H_2O$, yields water as a product, it is reasonable to propose that glycol–water phase separation occurs predominantly in the surface regions of the growing spheroidal morphologies, and is responsible for the observed additional surface designs.

Support for the liquid crystal microemulsion templating model stems from similar kinds of reactions that have recently been performed using other alkylammonium dihydrogen-phosphate–glycol and oil–TEG–water–DDP synthesis mix-
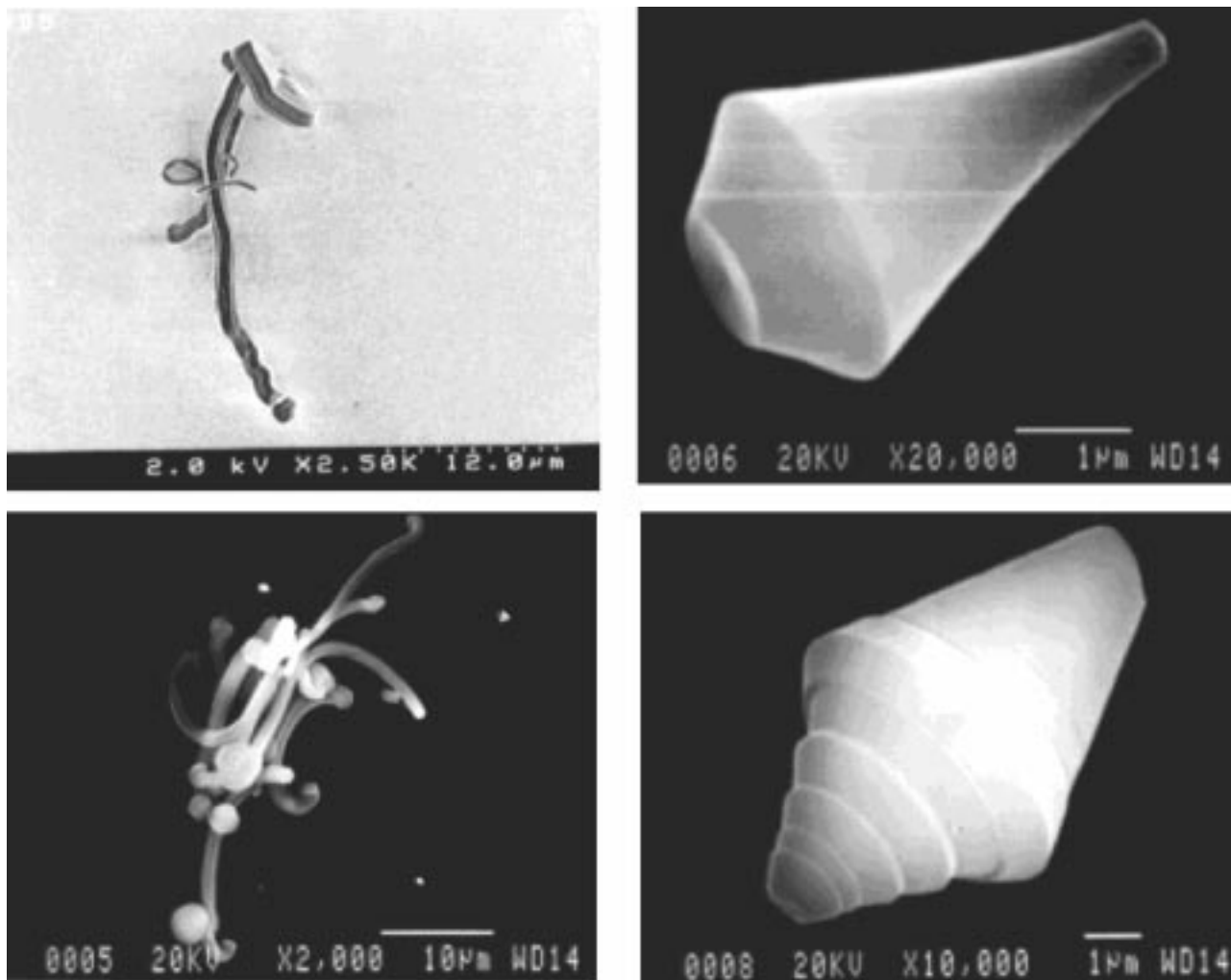
Fig. 4 Scanning electron microscopy images of representative low and high curvature mesoporous silica synthetic morphologies

tures.[26] They too give rise to interesting shell-shapes, with intricate cellular designs located on the internal and external surfaces of these morphologies, Fig. 1(*b*).

Silicate Liquid Crystals

Quiescent, acidic, dilute and homogeneous solution phase conditions are the key ingredients for morphogenesis of shape in the mesoporous silica system.[14] The PXRD patterns and the [29]Si magic-angle spinning nuclear magnetic resonance (MAS-NMR) spectra collected for representative mesoporous silica morphologies are those expected for hexagonal mesoporous silica, MCM-41.[12] Scanning electron microscopy images of large populations of morphologies, obtained by reaction-profiling a broad range of synthesis conditions by varying acidity, concentration and temperature, reveal the existence of certain size domains and basic forms,[14] Fig. 4. The overall dimensions of the morphologies can be varied between *ca.* 1 and 70 μm and their shape can be changed from low curvature fibers to high curvature discoids, gyroids and spirals. Transmission electron microscopy images of sectioned as well as complete morphologies define the spatial relationship between the hexagonal close-packed *ca.* 50 Å channel mesostructure and the overall macroscopic form, Fig. 5. The channels traverse the body length of the low curvature fibers while they coil concentrically around the body of the high curvature discoids and gyroids. The fact that TEM images can be obtained by directly imaging the samples (*i.e.* without sectioning) implies the existence of a high degree of spatial organization of the channels throughout the entire morphology. In addition, an atomic force microscope

(AFM) image of the surface of a gyroid revealed parallel stripes with a periodicity of *ca.* 90 Å twisting around the main axis of the morphology, Fig. 6. This surface mesostructure presumably represents a silicified recording of the termination of growth of the gyroid morphology.[15]

The mesostructure-morphology relationships established by SEM, TEM and AFM suggest the operation of a growth-driven curvature process of a self-organizing silicate liquid crystal seed, rigidifying through polymerization, Fig. 7. The curvature may originate through polymerization-induced contraction stresses and/or non-linear reaction-diffusion growth. Fast axial growth of the seed with minimal curvature creates fiber-like forms. With increasing rates of axial curvature, the loop and toroidal morphologies begin to emerge. Discoids appear when concentric co-axial cylindrical growth is fast relative to axial growth. Gyroids, knots and spheroids likely emerge when this process is comparable to the rate of axial growth. (All of the mentioned names for the shapes are self-explanatory descriptions of particular morphologies.)

A switch in the growth process, involving a reaction-diffusion growth instability, bifurcation,[28] may be responsible for the observation of hybrids of low and high curvature forms, such as 'tadpole' and 'phone' shapes. These odd shapes might originate with changes between fast concentric and fast axial growth. It is significant that certain discoid shapes have better ordered central core regions than others. This suggests that more ordered discoids likely evolve from concentric outward growth from a fairly well structured silicate liquid crystal seed, while the poorer ordered ones emerge from the inward growth of a toroid.
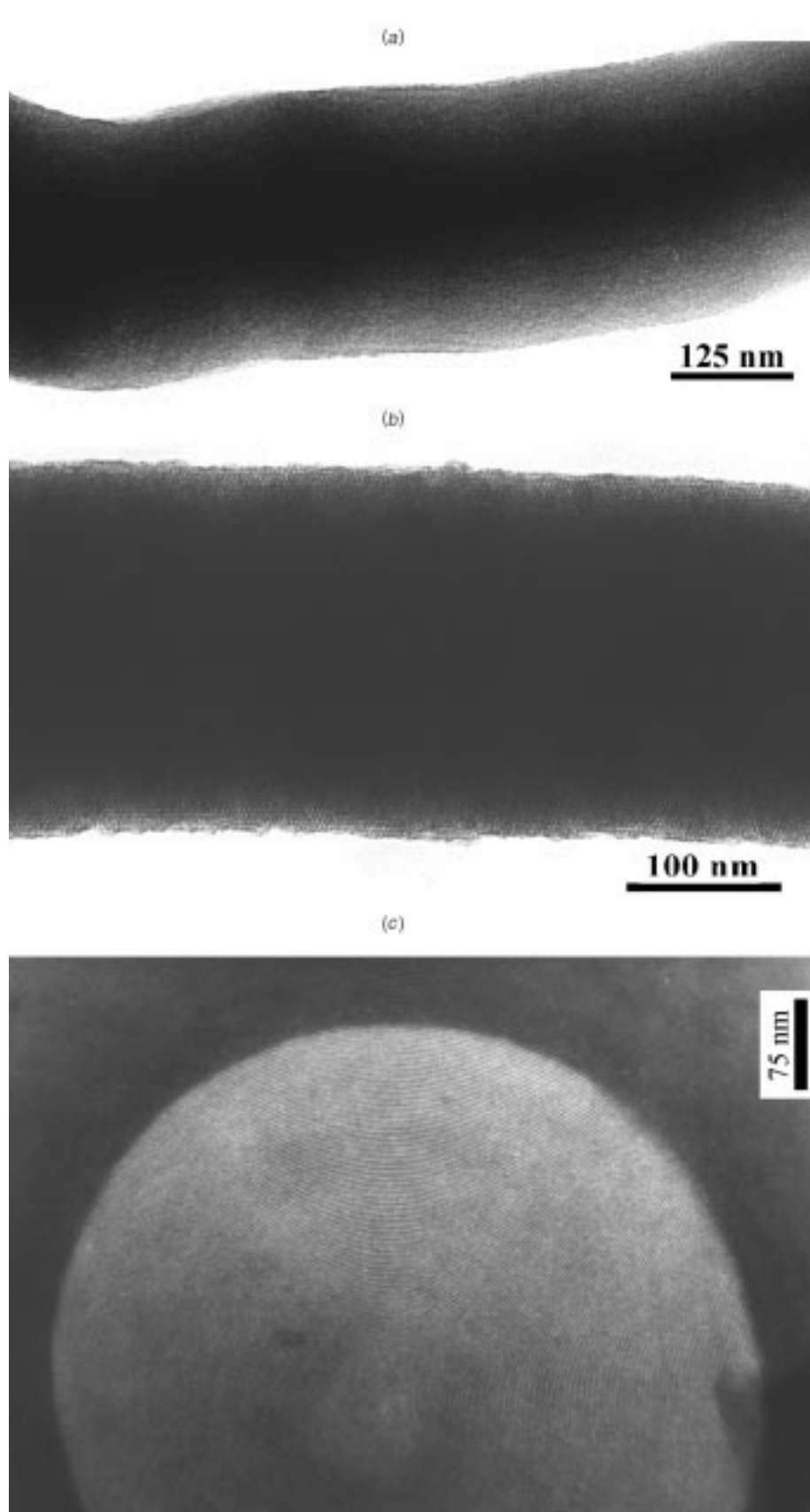
Fig. 5 Transmission electron microscopy images of representative whole mounted (*a*) rope, (*b*) gyroid and (*c*) discoid mesoporous silica morphologies. The mesoscale channels run down the axis of the rope, and whirl around the unique rotation axis of the gyroid and discoid

Morphogenesis of Silica and Aluminophosphate Shapes

The combined results of the silica and aluminophosphate systems provide an entry into the size and shape control of inorganic morphologies. The surface patterns in the silica and aluminophosphate morphologies may not have a common origin for the pattern generation process. However, when taken together with knowledge of the spatial relationship between the mesostructure and the overall form, a first principles model

for morphogenesis can be developed. Fig. 7 summarizes our current understanding of the morphogenesis of shape and the origin of surface decorations, in both the silicate and phosphate liquid crystal systems. For the silica morphologies, surface waves[29,30] and non-linear reaction-diffusion[28] are possible mechanisms for the surface patterning while for the organo-thermally prepared aluminophosphates, phase separation is a possible candidate.[31,32]

The Shape of Things to Come

With the ability to synthesize inorganic materials with intricate forms, a question now arises as to why shape these materials? In
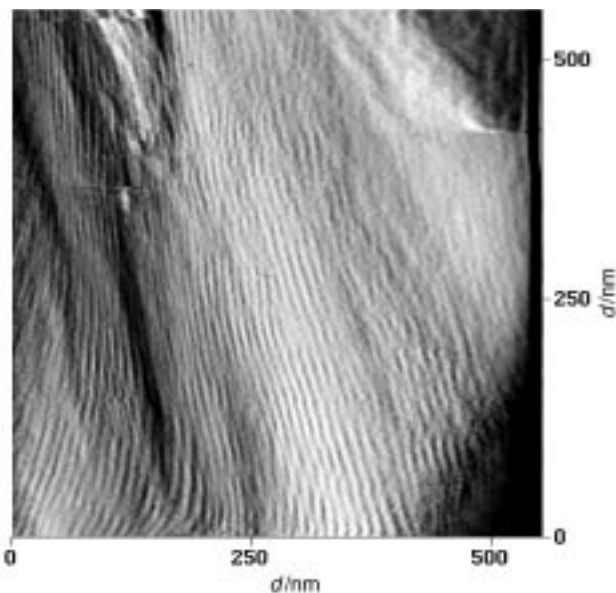

Fig. 6 Atomic force microscopy image of the surface of a gyroid mesoporous silica morphology displaying a surface mesostructure that whirls around the unique rotation axis of the gyroid and mirrors the underlying bulk mesostructure

the context of mesoporous silica, it is interesting to glance at some recent developments that take advantage of this knowledge. The motivation behind these experiments derives from the notion that the control of morphology and texture is the mainstay of materials science, particularly for tuning mechanical, magnetic, electronic, optical, separation and catalytic properties of materials.

Supported and free-standing mesoporous silica films

The templating of mesoporous silica films at surfactant structured solid–water and air–water interfaces has recently been reported.[22,23,33–35] In brief, mesoporous silica films, *ca.* 1–10 micron in thickness, could be deposited on the base of a horizontally held mica substrate under static conditions. Scanning electron microscopy studies of the early stages of film formation revealed that the mesoporous silica nucleates as thin ribbon patterns that are aligned with the mica substrate, Fig. 8, which then later expand in size and coalescence into extended sheet-like structures. Other substrates have subsequently been studied including graphite[35a] and gold.

In the case of soluble surfactants like CTACl (cetyltrimethyl-ammonium chloride), structures involving hemimicelle overlayers are known to exist at the air–water interface.[36–38] With this knowledge, mesoporous silica films with a thickness up to *ca.* 1–10 micron were readily formed at the air–water interface, under static conditions, with reaction time ranging from minutes to days.[34] Scanning electron microscopy and TEM images of the films reveal that they are continuous, contain very well ordered and oriented channels, Fig. 9.

The availability of free-standing as well as supported mesoporous silica films on a range of substrates including mica, graphite, silica and gold provides new and exciting opportunities for tailoring pore architecture, composition, adsorption properties and surface reactivity. The films have the potential to be used as membranes in large molecule catalysis, separation science and chemical sensor technology, as well as masks and molds for nanolithography and nanostructured materials.
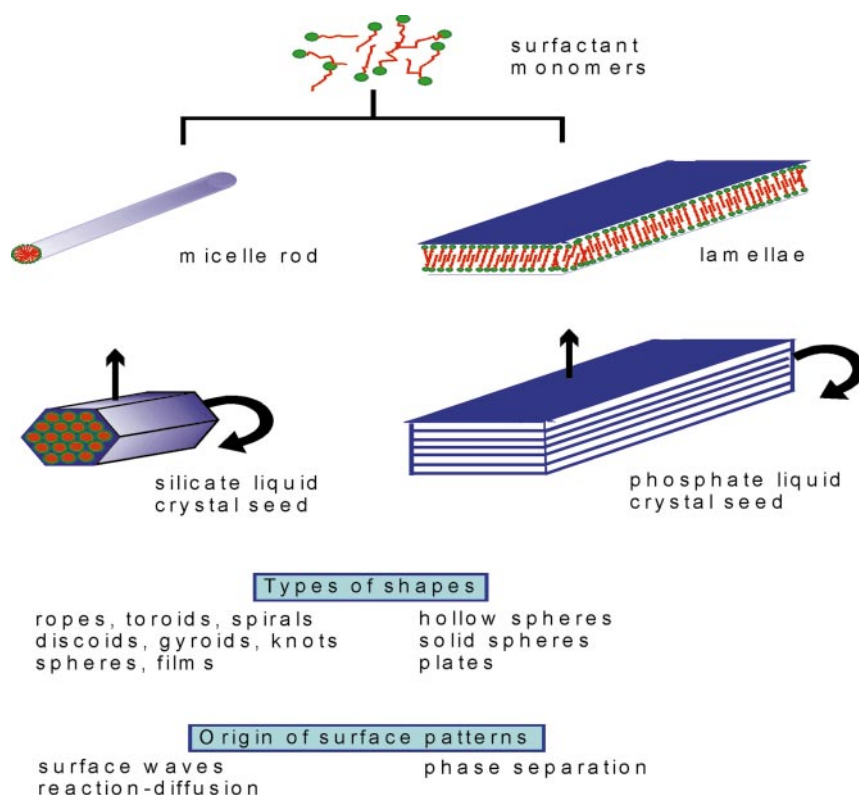

Fig. 7 Illustration of the current understanding of the morphogenesis of shape and the generation of surface patterns in the silicate liquid crystal templated mesoporous silica and phosphate liquid crystal templated mesolamellar aluminophosphate systems. Arrows indicate the primary growth direction of the seeds
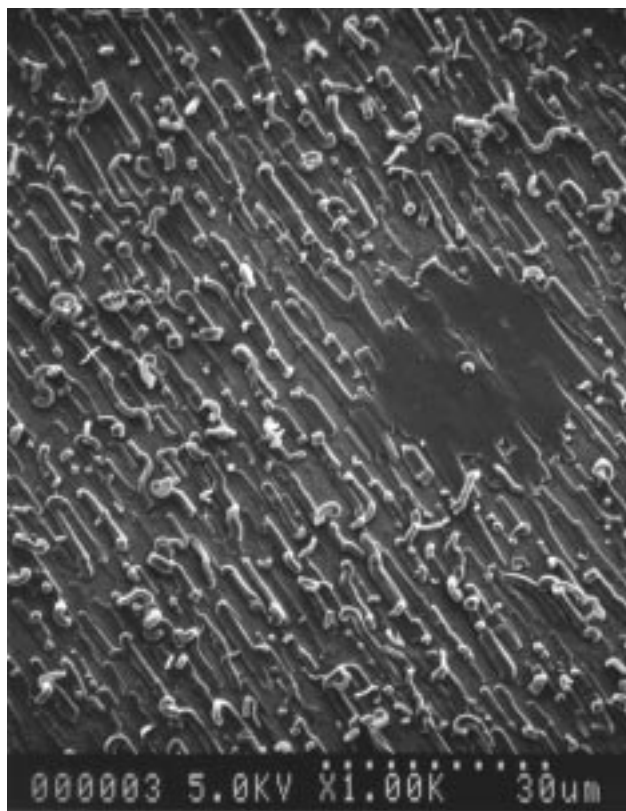
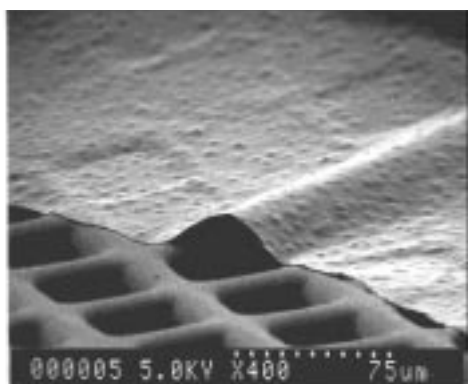**Fig. 8** Scanning electron microscopy image of the nucleation and growth of a mesoporous silica film on mica

Fig. 9 Scanning electron microscopy (top) and TEM (bottom) images of a free-standing mesoporous silica film grown at the air–water interface

Macroscale designs of mesostructured silica; self-assembled monolayer (SAM) and vesicle templates

SAM templates. The modification of surfaces by ultraviolet and X-radiation, ion and electron beams, microcontact printing, and lithographic molding technologies provide patterned structures of sub-micrometer dimensions for a variety of device applications. Self-assembly of alkanethiols on gold surfaces allows a convenient route to selected area deposition of materials, as diverse as polymers, proteins, ceramics and
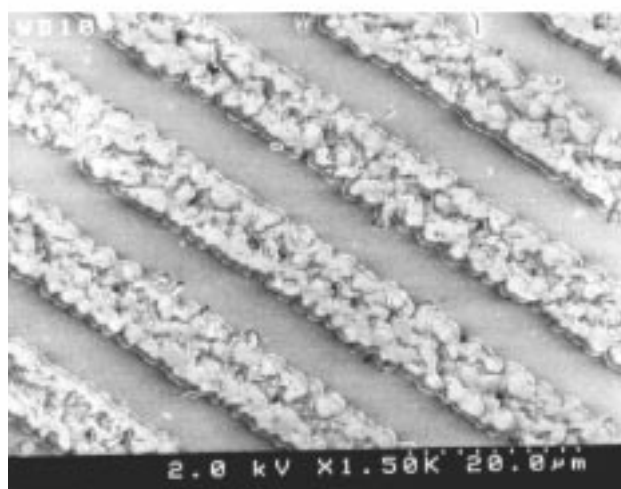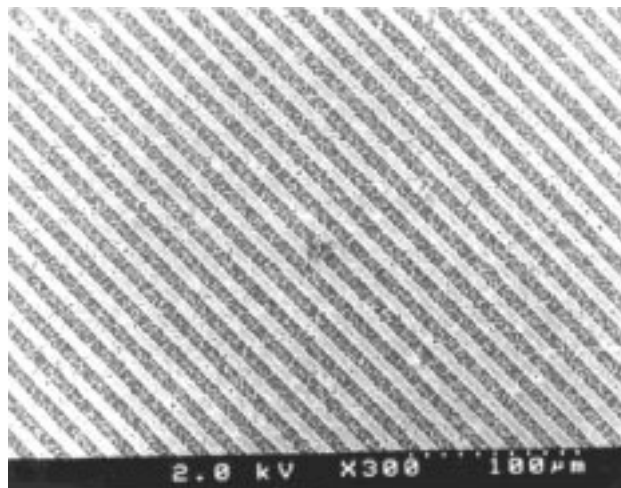

Fig. 10 Scanning electron microscopy images of mesoporous silica selectively grown on a parallel line pattern of hexadecanethiolate SAM on a gold substrate at low (top) and high (bottom) magnifications, respectively

semiconductors.[39–41] A novel 'three-way-templating' strategy is described here that facilitates the selected area growth of patterned mesoporous silica films. The process involves co-assembly of alkanethiolate decorated gold surfaces, surfactant–alkanethiolate hetero-bilayers and surfactant–silicate assemblies.[42]

Studies were initially performed with deposition of mesoporous silica on gold and hexadecanethiolate SAM coated gold. Scanning electron microscopy results displayed mainly disc- and ribbon-shaped structures which then showed signs of coalescence with increasing coverage. Powder X-ray diffraction patterns for the deposited material displayed an intense (100) low angle reflection corresponding to a d-spacing in the range of 35–38 Å, along with a much weaker (200) reflection. These were attributed to the oriented hexagonal form of mesoporous silica.

This synthesis procedure was then applied to the deposition of mesoporous silica onto a hexadecanethiolate SAM patterned gold substrate.[42a] Representative SEM images for the deposited material are shown in Fig. 10. The characteristic disc- and ribbon-shaped morphology of the mesoporous silica appeared to be predominantly deposited on the SAM patterned lines of the gold surface. Use of a hybrid patterned–unpatterned SAM established that the mesoporous silica preferentially deposits on the alkanethiolate regions of the gold. The corresponding PXRD pattern portrayed low angle (100) and (200) reflections (d_{100}-spacing of *ca.* 35 Å) that were diagnostic of aligned mesoporous silica. Furthermore, selected area energy
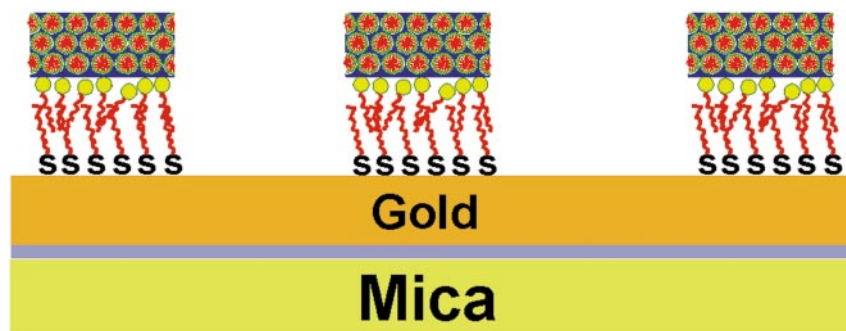
Fig. 11 Illustration (not drawn to scale) of the proposed 'three-way-templating' model for the selected area growth of the hexagonal form of mesoporous silica on the hexadecanethiolate SAM patterned regions of a gold substrate
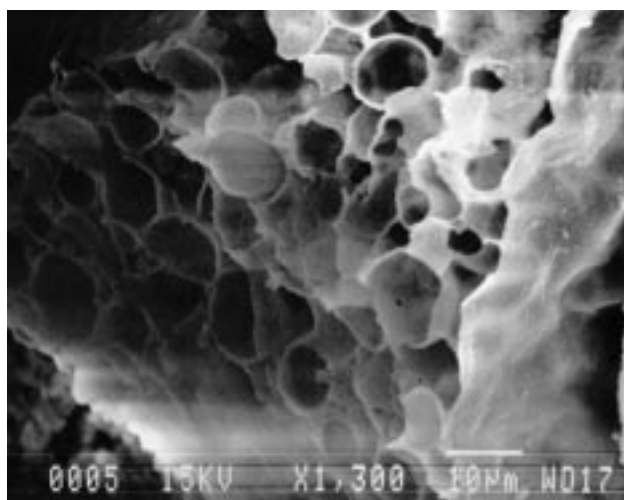

Fig. 12 Scanning electron microscopy image of a mesolamellar silica macroporous structure templated by mixtures of cationic didodecyldimethylammonium bromide and anionic sodium dodecyl sulfate surfactants in the vesicle region of the phase diagram

dispersive X-ray (EDX) analysis established the distribution of silicon in the mica–gold and mica–gold–SAM regions of the substrate. Quantification of the selectivity of the deposition process takes into account the different penetration depths of the electron beam in these two regions. It is important to note that the thickness of the gold overlayer on the mica is *ca.* 70 nm while the penetration of the electron beam under the conditions used can be at least 500 nm. The EDX results showed that greater than 80% of the deposited mesoporous silica was located on the SAM delineated regions of the substrate. This implied much greater selectivity in the rate of adhesion of silicate–micellar solute species to the SAM defined areas rather than to the bare gold itself. Transmission electron microscopy images were recorded for ultrathin cross-sections of the deposited silica and established the hexagonal symmetry form of the silica. In addition, these images displayed the average d_{100}-spacing and the preferred alignment of the channels approximately parallel to the surface, both of which correlated well with the PXRD results.

The proposed model for the selected area growth of mesoporous silica on SAM patterned gold is summarized in Fig. 11. The process for creating mesoporous silica with micron scale designs involves a unique kind of 'three-way-templating' in which hydrophobic interactions between the alkane tails of an alkanethiolate SAM on gold and those of cationic surfactants in aqueous solution are the driving force behind the spontaneous co-assembly of an alkanethiolate–surfactant hetero-bilayer. The association of surfactants with SAMs is well described by the Langmuir adsorption isotherm and provides credance for the hetero-bilayer templating proposal.[42b] The externally arranged polar trimethylammonium head groups of the hetero-bilayer (exposed to the aqueous solution phase) act

as adherent hydrophilic sites that preferentially accrete silicate–surfactant micellar solute species and form mesoporous silica in the SAM coated gold regions of the substrate. Perceived uses for mesoporous films having macroscale designs of mesopores include sensors, membranes, integrated electronics and biomedical devices.

Vesicle templates. Biosilicification of silicate–organic co-assemblies produces shapes such as diatoms and radiolaria microskeletons.[1] The diversity of patterns on these silica skeletons has defied explanation in terms of biological form and function. As described above and in the context of biomimetics, the chemistry of silica was recently taken to new heights when lyotropic silicate liquid crystal hexagonal, cubic and lamellar mesophases were transformed to replica silica mesostructures.[12] With this new synthetic paradigm, periodic patterns of ångström precision tunable voids could be imprinted into silica in the mesoscopic size range of 20–100 Å. The methodology enabled the morphology of mesoporous silica to be controlled over all three spatial dimensions to produce fibres, films and a myriad of curved forms.[14,15,20,22,33–35,43] In this same vein, the surfactant structured interfaces of microemulsions have been effectively used to mold mesoporous silica into solid and hollow sphere shapes,[23,24] while SAM templates facilitate the growth of micron scale patterns of mesoporous silica.[42a] While the length scale of surfactant micelles is ideal for templating regular patterns of mesopores in silica the currently achievable size range has a natural upper limit of around 100 Å. To escape from this constraint, yet still utilize the templating ability of surfactants, necessitates another paradigm shift.

Here a vesicle-based synthesis of macroporous forms of silica is described.[44] Integral to the study is the knowledge that mixtures of oppositely charged cationic and anionic surfactants can develop stable and narrow dispersions of vesicles under mild aqueous conditions.[45] One such example that has been cited is in the didodecyldimethylammonium bromide (di-DDAB), sodium dodecyl sulfate (SDS) and water phase diagram. The di-DDAB:SDS:H₂O ratio provides considerable scope for tailoring surface charge, curvature, size, dispersion, permeability and aggregation properties of the vesicles, and the transcription of this information into the silica replica.

A typical synthesis employs tetraethyl orthosilicate and hydrochloric acid along with the aforementioned ternary phase system. Scanning electron micrographs of the resulting product consisted of a honeycomb-like macrostructure with roughly 5–10 micron scale pores and *ca.* 1 micron thick silica dividing walls, Fig. 12. Powder X-ray diffraction patterns of the honeycomb morphology and TEM images of microtomed sections showed that the silica walls could be pH and compositionally tuned in a synthesis, from mesolamellar with a d-spacing of *ca.* 30 Å to amorphous. Control syntheses containing di-DDAB or SDS produced solely mesolamellar and amorphous forms of silica respectively, with particulate non-descript morphologies.

In the determination of a growth model for these micron scale silica honeycombs, it is surmised that cation–anion sur-

Fig. 13 Transmission electron microscopy image (heavy-metal negative staining methodology) of poly(phenol–formaldehyde) mesofibre bundles templated by mesoporous silica molds. The diameter of the individual fibres constituting the bundles is about 30 Å

factant pairs behave as zwitterionic surfactants and produce vesicles spontaneously without the need for mechanical or chemical perturbations to the system. The surfactant concentrations that favor vesicles are only a few percent and are limited by their close-packing. It is likely that the silica honeycombs emerge from the interfacial silicification of contiguous aggregations of silicate–di-DDAB–SDS multilayer vesicles in much the same way that Thompson[46] imagined radiolaria formed from the deposition of silica in the spaces within a protoplasmic froth. This proposal receives support from the direct optical microscopy observation of vesicles in di-DDAB–SDS–H$_2$O mixtures before the addition of tetraethyl orthosilicate.

As numerous single- and double-tailed surfactants with opposite charges are reported to form equilibrium vesicles spontaneously, there is considerable scope for the synthesis of new silica morphologies. This provides an opportunity to further the understanding of biological silicification and for tailoring macroporous forms of silica in materials chemistry to separate colloids, bacteria, viruses, polymers and biomolecules.

Mesomolding

Ever since the discovery of the MCM41S family of materials[12] a great deal of interest has been generated in various aspects of these materials including the mechanism of formation, variation of pore sizes through a variety of techniques, tuning the framework composition, and employing the internal channels as mini-reactors for fabricating diverse forms of mesostructures.[27] However, there has been a simple question that has remained unanswered, namely: what really is the length and internal architecture of the channels of the mesoporous silicas synthesized under different conditions?

Here, we present work performed in using the channels of mesoporous silica as mesomolds to create a polymer replica.[43] Extraction of the polymer mesofibres intact allows high resolution microscopy studies of their structure and hence a novel

process for the synthesis of controlled diameter polymer mesofibres. An added benefit with additional microscopy could be an insight into the length and perhaps even the presence of constrictions in the channels, holes in the channel walls, and other channel defects.

The synthesis involves acid-catalyzed polymerization of intra-channel phenol and formaldehyde to create a poly-(phenol–formaldehyde) channel mold. This is followed by mild HF–H$_2$O dissolution of the surrounding mesoporous silica matrix and release of the encapsulated polymer. Powder X-ray diffraction analysis of the silica–polymer composite (before etching) displayed a pattern of low 2θ values that is characteristic of the hexagonal form of mesoporous silica. At a 2θ value of *ca.* 25°, a broad peak was observed suggesting the presence of disordered polymer in a glassy silica host matrix. Moreover, this peak was retained for the sample obtained after etching, characterizing the presence of an amorphous polymer. Elemental analysis on the silica–polymer composite sample gave 45% carbon content. For an ideal complete filling of the channels, the required carbon content was calculated to be 59%, and hence the channels may be assumed to be *ca.* 75% filled. This degree of mesopore filling is consistent with the results of 77 K N$_2$ adsorption isotherms recorded for calcined mesoporous silica before and after polymer encapsulation in the channels, which show that the accessible pore volume of the mesoporous silica has diminished by about 85 vol. %.

Transmission electron microscopy imaging of the extracted polymer fibers was performed on thin holey carbon film as well as with heavy-metal negative staining on an ultrathin carbon film (*ca.* 7 Å thick). The extracted polymer fibers were found to have aspect ratios that exceeded 10^3, indicating that the channels run continuously throughout the body of the micron dimension mesoporous silica host particles, Fig. 13. Both single and bunches of polymer strands were observed and the diameters of the polymer mesowires were all about 3 nm, comparable to the channel dimensions of the mesoporous silica host. Clearly, deposition of the polymer occurred selectively within the channels rather than on the external surface.

Control TEM experiments have been performed for bulk forms of poly(phenol–formaldehyde), as well as samples synthesized on the surface of non-porous Carbosil silica that had been pre-treated under identical conditions to those used for the mesoporous silica channel host material. The TEM images show distinct morphologies, that is, shapeless polymer particulates are extracted from the Cabosil and non-descript polymer agglomerates are obtained for the bulk form of the polymer. Polymer mesofibres of 30 Å are extracted only from the mesoporous silica molds.

While it is apparent that the method can generate polymer mesofibres, the achievable TEM resolution is unfortunately degraded by the poor electron beam stability and unfavourable electron contrast from the C/H/O light elemental composition. This has so far prevented the elucidation of the precise form of the mesowires. Heavy-atom labeling of the poly(phenol–formaldehyde) and high contrast inorganic polymers are being explored to overcome this problem. Nevertheless, the paradigm of replicating the channels of mesoporous silica provides a synthetic route to a diversity of polymer, ceramic, semiconductor, and metallic mesowires with a range of compositions and properties. Technologies based on tunable diameter mesofibres could emerge as a result of this work.

Mesoporous silica spheres

An extraordinary gyroid-to-sphere shape transition has been unveiled in the growth of mesoporous silica morphologies under quiescent acidic synthesis conditions.[14,15,47] It can be induced by just a slight increase in the pH of a surfactant-based gyroid preparation.[14] As the acidity is gradually dropped from the gyroid domain, the growth process changes from one involv-
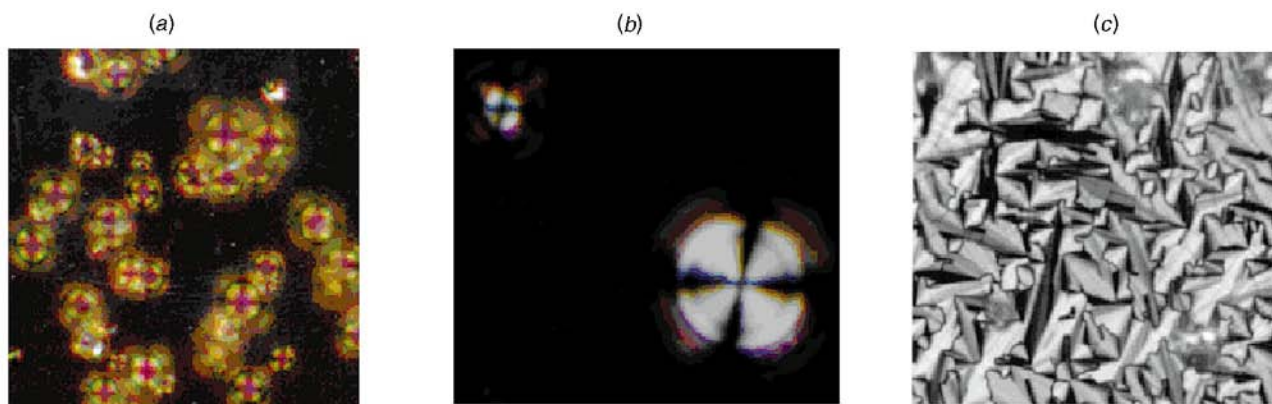
Fig. 14 Optical images of mesoporous silica between crossed polarizers (a) spheres, (b) discoids, (c) free-standing film
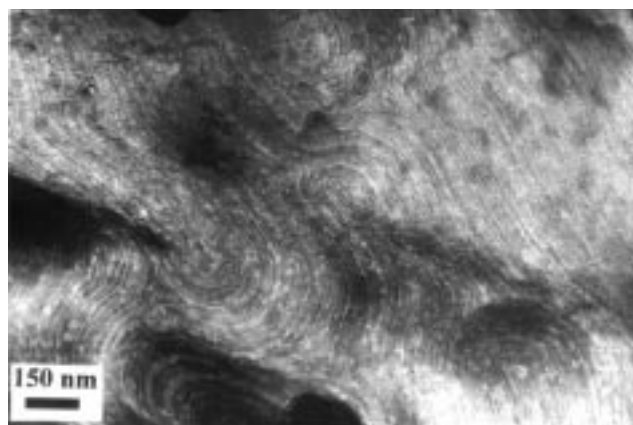

Fig. 15 Transmission electron microscopy image depicting the liquid crystalline channel texture observed for mesoporous silica films synthesized at the boundary between air and water

ing a smooth continuous deposition of silicate–surfactant micellar solute species onto specific regions of an evolving silicate liquid crystal seed, to one in which deposition occurs randomly and in non-specific regions of the seed. This creates rounded multi-granular gyroidal morphologies which develop into sphere shapes with smooth surfaces. The gyroid-to-sphere metamorphosis appears to correlate with a pH dependent switch in the mode of formation of these high curvature morphologies, from the gyroid involving fast and local polymerization of a growing silicate liquid crystal seed, to the sphere based upon slow and global polymerization of a silicate liquid crystal droplet. Surface tension will drive the shape of a soft silicate liquid crystal droplet to adopt the shape of a sphere, ultimately to be rigidified as a mesoporous silica sphere. When viewed in an optical microscope and between crossed polarizers, they display an intense and clear colored hyperbolic-cross whose curvature varies from sphere to sphere,[48] Fig. 14(a).

In materials science where the morphology of mesoporous inorganic materials is likely to determine their function, this paradigm is expected to have wide ranging technological implications. Specifically, the ability to synthesize 1–15 micron diameter mesoporous silica spheres with a narrow sphere size distribution portends a myriad of applications in for example, large molecule catalysis and chromatographic purification of mixtures of biomolecules. The size and shape of mesoporous spheres are expected to be crucial when designing optimum macromolecule catalysis and separation systems.

Role of Defects in Inorganic Liquid Crystals

It is well documented that defects have a profound impact on the properties of solid-state materials, such as, the nucleation and growth of crystals, bulk and surface reactivity, ionic and electrical charge transport, and mechanical properties. There-

fore, it should come as no surprise that the effect of defects on the properties of liquid crystals is equally dramatic.[48,49] In this section we briefly consider the role of defects in inorganic liquid crystals, particularly with respect to their possible effect on influencing the morphology and channel plans of mesoporous silica films and forms.[47]

By contrast with the submicroscopic dimensions of defects in the solid state, those of liquid crystals are often microscopic in size. As a result, the energy required for stabilizing defects in liquid crystals is much less than in solid crystals and leads to defects with larger dimensions and stronger distortions of the director fields. Surface interactions are of special importance, as they can lead to the stabilization of particular types of defects in liquid crystals. Defects as well as electric or magnetic fields, temperature gradients and stress fields can play a determining role in the growth processes of liquid crystals. Point defects, linear defects, and two-dimensional defects of various types are found to exist in liquid crystals and occur in higher concentrations than in solids due to the higher mobility of the constituent molecules.

Liquid crystals usually possess a low viscosity and can be deformed by small external forces. Within this definition, liquid crystals act as an elastic medium. The deformations and director field configurations can be treated by elastic continuum theory and is the approach most often used to calculate director field configurations in liquid crystal films and droplets.[48,49] The director profile is obtained by minimizing the free-energy functional of elastic (i.e., splay, bend, twist distortions), surface and field forces in the liquid crystal. The patterns of stable director fields depend on the bulk and surface elastic constants, anchoring strengths at the polar surface (i.e., homogeneous and homeotropic interactions), magnitudes of applied electric and magnetic fields, and surface to volume ratio of the liquid crystal. It is the pattern of director fields and degree of orientational order that give rise to the characteristic textures of liquid crystals when viewed between crossed polars in a polarizing optical microscope. Briefly, the textures originate from the interference of the doubly refracted ordinary and extraordinary light rays which experience different phase shifts after passing through the birefringent liquid crystal medium. The calculated optical interference patterns for various types of director fields for films and droplets, in different orientations with respect to the direction of the crossed polars, are quite distinct and have been successfully used to unveil the nature of orientational order in liquid crystals.[48,49]

The picture that is emerging from continuing studies of the morphogenesis of shape in hexagonal mesoporous silica films and forms is that a relation does exist between a particular morphology and the choice of synthesis conditions, the use of a quiescent versus a dynamic solution environment and the growth, polymerization and curvature of a silicate liquid crystal seed. Furthermore, the role of defects in silicate liquid crystals, in determining the shape and channel plans of hexagonal meso-

porous silica that are grown in one-, two- and three-dimensions, is becoming increasingly apparent. Dramatic examples of the affect of such defects are seen through the optical birefringence properties and TEM images of mesoporous silica discoid morphologies and free-standing films,[47] Fig. 14. For instance, the discoid shapes with concentric co-axial liquid crystal channel plans, Fig. 5(c), may be initiated by a topological defect in a precursor silicate liquid crystal seed, comprised of a circular symmetry director field around a disclination line with strength $s = +1$ and additive constant angle $\varphi = \pi/2$.[48,49] Thus, discoids are expected when concentric co-axial cylindrical growth is fast compared to the rate of axial growth around the central disclination line defect, while gyroids emerge when the whirling growth process is comparable to the rate of axial growth. In a similar vein, various kinds of linear defects are most likely responsible for the emergence of the observed swirling and curling channel plans that have recently been observed in free-standing mesoporous silica films, Fig. 15.[35b]

Conclusion: Past, Present and Future

The science of morphogenesis at the present date has been a cumulation of extensive work by several pioneers over the past 150 years. In 1873, Harting[50] published an article on synthetic morphology in which he described how calcareous concretions with 'natural' form could emerge from the mixing of calcium and phosphate or carbonate ions in a complex biological milieu, like albumen. More than a century later Lowenstam[3] in 1981 documented the composition and distribution of mineral forms in biological systems and pronounced his theory of how the accretion of inorganics by organics is able to shape minerals into intricate morphologies. In 1952, stimulated by the visual imagery of natural shapes, Turing[51] developed a theory of how patterns can appear spontaneously in chemical reaction-diffusion systems that are far from equilibrium. Turing's contributions proved relevant to the understanding of morphogenesis, and suggested to developmental biologists that these kinds of chemical processes might be responsible for the appearance of complex patterns in nature. Since the publication of Turing's influential work there has been intense activity on the mathematical modeling of patterns in biological and non-biological systems.[28]

Also integral to the present understanding of morphogenesis was the discovery by Reinitzer[52] in 1888 of organic liquid crystals. These materials presented a striking example of self-organization. Lehmann's 1911 book[52] provided then the earliest description of the properties of organic liquid crystals and laid down the foundation of how they could be considered as intermediate between that of living and non-living matter. About a century ago, Haeckel,[53] in his last book *Crystal Souls, Studies of Inorganic Life*, wrote that the properties of organic liquid crystals were somehow connected with radiolaria microskeletal forms. Now *inorganic* liquid crystals are producing synthetic morphologies with 'natural' form. Just as an understanding of soft-matter in living systems depended on a molecular level understanding of DNA and its interaction with proteins, the hard-matter problem demands the same level of comprehension of the involvement of inorganic ions and solids in biological systems.[7]

This discovery of 'purely' synthetic shape through the mineralization of inorganic liquid crystals[13,14] has provided interest in 'morphosynthesis'.[5] Inorganic liquid crystals, especially the unique kind of self-organization and mineralization which they exhibit, provide a new tool for enhancing the understanding of the form problem. Emerging from this work is a chemical basis for the language of inorganic shape. While morphogenesis was originally motivated by Darwinian theories of evolution, morphosynthesis is now driven by the evolution of a materials society. The control of morphology is expected to play a central role in the development of new materials, products and processes.

The future looks bright for morphosynthesis in inorganic materials chemistry, especially studies of inorganic liquid crystals as blueprints for inorganic materials with 'natural' form. The last statement in Harting's 1873 synthetic morphology paper insightfully points to the future of biomimetic inorganic materials chemistry: "*this is a large field with many opportunities, there is much work to be done, and we have taken but the first step.*".[50]

Acknowledgements

References

1 *Biomineralization: Chemical and Biochemical Perspectives*, eds. S. Mann, J. Webb and R. J. P. Williams, VCH Publishers Inc., New York, 1989.
2 *Biomimetic Materials Chemistry*, ed. S. Mann, VCH Publishers Inc., New York, 1996.
3 H. A. Lowenstam, *Science*, 1981, **211**, 1126.
4 S. Mann and G. A. Ozin, *Nature* (*London*), 1996, **382**, 313.
5 G. A. Ozin, *Acc. Chem. Res.*, 1997, **30**, 17.
6 S. Mann and D. Walsh, *Chem. Br.*, 1996, **32**, 31.
7 *The Biological Chemistry of the Elements*, *The Inorganic Elements of Life*, eds. J. J. R. Fraústada da Silva and R. J. P. Williams, Clarendon, Oxford, 1993.
8 J. Klinowski, A. L. Mackay and H. Terrones, *Philos. Trans. R. Soc. London, Ser. A*, 1996, **354**, 1975.
9 *Morphology of Crystals*, *Part A*, ed. I. Sunagawa, Terra Scientific Publishing Company, Tokyo, 1987.
10 A. L. Mackay, *THEOCHEM*, 1995, **336**, 293.
11 A. L. Mackay, *Curr. Sci.*, 1995, **69**, 151.
12 C. T. Kresge, M. Leonowicz, W. J. Roth, J. C. Vartuli and J. C. Beck, *Nature* (*London*), 1992, **359**, 710.
13 (*a*) S. Oliver, A. Kuperman, N. Coombs, A. Lough, G. A. Ozin, *Nature* (*London*), 1995, **378**, 47; (*b*) S. Oliver, A. Lough, G. A. Ozin, unpublished work.
14 H. Yang, N. Coombs and G. A. Ozin, *Nature* (*London*), 1997, **386**, 692.
15 G. A. Ozin, H. Yang, I. Sokolov and N. Coombs, *Adv. Mater.*, 1997, **9**, 662.
16 S. Oliver and G. A. Ozin, *Adv. Mater.*, 1995, **7**, 943.
17 S. Oliver, N. Coombs and G. A. Ozin, *Adv. Mater.*, 1995, **7**, 931.
18 H.-P. Lin and C.-Y. Mou, *Science*, 1996, **273**, 765.
19 G. A. Ozin, D. Khushalani and S. Oliver, *in NATO Adv. Res. Workshop Proc.: Modular Chemistry*, ed. J. Michl, Aspen, Colorado, 1995.
20 G. A. Ozin, D. Khushalani and H. Yang, in *NATO Adv. Res. Workshop Proc: Supramolecular Chemistry*, ed. J. Wuest, Val Morin, Quebec, 1996.
21 A. Chenite, Y. Le Page, V. R. Karra and A. Sayari, *Chem. Commun.*, 1996, 411.
22 I. A. Aksay, M. Trau, S. Manne, I. Honma, N. Yao, L. Zhou, P. Fenter, P. M. Eisenberger and S. M. Gruner, *Science*, 1996, **273**, 892.
23 S. Schacht, Q. Huo, I. G. Voigt-Martin, G. D. Stucky and F. Schüth, *Science*, 1996, **273**, 768.
24 Q. Huo, J. Feng, F. Schüth and G. D. Stucky, *Chem. Mater.*, 1997, **9**, 14.
25 P. T. Tanev and T. J. Pinnavia, *Science*, 1996, **271**, 1267.
26 S. Oliver and G. A. Ozin, unpublished work.
27 G. J. Gainsford, N. B. Kemmitt and N. B. Milestone, *Inorg. Chem.*, 1995, **34**, 5244.
28 *Chemical Waves and Patterns*, eds. R. Kapral and K. Showalter, Kluwer Academic Publishers, Dordrecht, 1995.
29 M. Jacob, K. Larsson and S. Z. Andersson, *Kristallogr.*, 1997, **212**, 5.
30 M. Jacob, K. Larsson and S. Z. Andersson, *Kristallogr.*, 1996, **211**, 875.
31 *The Colloidal Domain where Physics, Chemistry, Biology and Technology Meet*, D. F. Evans, Wennerström , VCH Publishers Inc., New York, 1994.
32 J. N. Israelachvili, *Intermolecular and Surface Forces*, Academic, New York, 2nd edn., 1991.
33 H. Yang, A. Kuperman, N. Coombs, S. Mamiche-Afara and G. A. Ozin, *Nature* (*London*), 1996, **379**, 703.

34 H. Yang, N. Coombs, I. Sokolov and G. A. Ozin, *Nature* (*London*), 1996, **381**, 589.
35 (*a*) H. Yang, N. Coombs, I. Sokolov and G. A. Ozin, *J. Mater. Chem.*, 1997, **7**, 1285; (*b*) H. Yang, N. Coombs, Ö. Dag, I. Sokolov and G. A. Ozin, *J. Mater. Chem.*, 1997, **7**, 1755.
36 J. Böcker, M. Schlenkrich, P. Bopp and J. Brickmann, *J. Phys. Chem.*, 1992, **96**, 9915.
37 J. R. Lu, Z. X. Li, J. Smallwood, R. K. Thomas and J. Penfold, *J. Phys. Chem.*, 1995, **99**, 8233.
38 R. K. Thomas and J. Penfold, *Curr. Opin. Colloid Interface Sci.*, 1996, **1**, 23.
39 E. Kim, Y. Xia and G. M. Whitesides, *Adv. Mater.*, 1996, **8**, 245.
40 A. Kumar, N. L. Abbott, E. Kim, H. A. Biebuyck and G. M. Whitesides, *Acc. Chem. Res.*, 1995, **28**, 219.
41 X. M. Zhao, Y. Xia and G. M. Whitesides, *Adv. Mater.*, 1996, **8**, 837.
42 (*a*) H. Yang, M. Coombs and G. A. Ozin, *Adv. Mater.*, 1997, **9**, 811; (*b*) G. B. Sigal, M. Mrksich and G. M. Whitesides, *Langmuir*, 1997, **13**, 2749.
43 S. Johnson, D. Khushalani, G. A. Ozin, T. Mallouk and N. Coombs, unpublished work.
44 G. C. Shen, N. Coombs and G. A. Ozin, unpublished work.
45 M. T. Yatcilla, K. L. Herrington, L. L. Brasher, E. W. Kaler, S. Chiruvolu and J. A. Zasadzinski, *J. Phys. Chem.*, 1996, **100**, 5874.

46 D'A. W. Thompson, *On Growth and Form: The Complete Revised Edition*, Dover Publications, Inc., New York, 1992.
47 H. Yang, N. Coombs, I. Sokolov, G. Vovk and G. A. Ozin, unpublished work.
48 *Liquid Crystals in Complex Geometries Formed by Polymer and Porous Networks*, eds. G. P. Crawford and S. Zumer, Taylor & Francis Ltd., London, 1996.
49 D. Demus and L. Richter, *Textures of Liquid Crystals*, Verlag Chemie, New York, 1982.
50 P. Harting, *Naturrkd. Voordr.*, 1873, **13**, 1.
51 A. M. Turing, *Philos. Trans. R. Soc. London, Ser. B*, 1952, **327**, 37.
52 F. Reinitzer, *Monatsh. Chem.*, 1888, **9**, 421; O. Lehmann, *Die Flussige Kristalle*, Akademische Verlags-gesellshaft M.B.H., Liepzig, 1911.
53 E. Haeckel, *Crystal Souls: Studies of Inorganic Life*, University of Jena, 1917.